Water Resources and Industry 35 (2026) 100332

Contents lists available at ScienceDirect

Water Resources and Industry

journal homepage: www.elsevier.com/locate/wri

Techno-economic evaluation of maximizing minimum liquid discharge from seawater desalination for the fertilizer industry

Nikhil Dilip Pawar [a,*], Carmelo Morgante [b], Thomas Pregger [a], Patrick Jochem [a]

[a] German Aerospace Center (DLR), Institute of Networked Energy Systems, Curiestr. 4, 70563, Stuttgart, Germany
[b] Department of Chemistry and Bioscience, Aalborg University, Fredrik Bajers Vej 7H, Aalborg Øst, 9220, Denmark

ARTICLE INFO

Keywords:
Decarbonization
Green hydrogen
Urea
Brine valorization
Zero liquid discharge
ZLD
MENA

ABSTRACT

The Middle East and North Africa region faces critical water scarcity and food security challenges that threaten economic development. Fertilizer use supports food self-sufficiency, but its production is highly water intensive. Supplying desalinated water to a decarbonized fertilizer plant offers an environmentally sustainable pathway.

This study investigates co-locating a decarbonized fertilizer plant with a seawater desalination facility, optionally implementing minimum liquid discharge (MLD) to generate additional revenue through recovery of magnesium hydroxide and sodium chloride (NaCl). Three configurations were modeled: a conventional seawater reverse osmosis (SWRO)-based plant; and two MLD configurations using high-pressure RO (HPRO), osmotically-assisted RO (OARO), and crystallizers. Financial performance was assessed using a novel discounted and allocated levelized cost (DALC) method, internal rate of return (IRR), and net present value (NPV).

In a Moroccan case study, the conventional configuration achieved the lowest DALC and energy consumption (0.70 USD/m^3_{water} and 3.8 KWh_{el}/m^3), with an IRR of 23.9 %. The first MLD configuration had higher costs (0.94 USD/m^3_{water}, 12.0 KWh_{el}/m^3) and a lower IRR (14.5 %), with water recovery limited to 71.4 % due to nonuse of magnesium crystallizer effluent (60.4 % in the conventional setup). Reusing this effluent in the second MLD configuration increased water recovery to 96.7 %, yet higher impurities at the NaCl crystallizer feed reduced the IRR to 9.7 %, which could be improved through financing strategies such as lowering capital costs to endorse the MLD-maximizing option.

The findings emphasize advancing impurity removal methods and exploring innovative project financing strategies to enable financially and environmentally sustainable seawater desalination for decarbonized fertilizer production.

Acronyms

Symbol	Description
BDC	Brine disposal cost
COGS	Cost of goods sold
CSSF	Crystallizer salinity scale-up factor
DALC	Discounted and allocated levelized cost

(*continued on next page*)

* Corresponding author. Curiestr. 4, 70563 Stuttgart, Germany.
E-mail address: Nikhil.Pawar@dlr.de (N.D. Pawar).

https://doi.org/10.1016/j.wri.2025.100332
Received 24 September 2025; Received in revised form 10 November 2025; Accepted 20 November 2025
Available online 26 November 2025

(*continued*)

Symbol	Description
DCF	Discounted cash flow
HPRO	High pressure reverse osmosis
IRR	Internal rate of return
IX	Ion exchange
$Mg(OH)_2$	Magnesium hydroxide
MLD	Minimum liquid discharge
NaCl	Sodium Chloride
NaOH	Sodium hydroxide
NF	Nanofiltration
NPV	Net present value
OARO	Osmotically-assisted reverse osmosis
SEC	Specific electricity consumption
SWRO	Seawater reverse osmosis
TEA	Techno-economic analysis
TPCF	Total project cash flow
TDS	Total dissolved solids
UPW	Ultrapure water
WACC	Weighted average cost of capital
ZLD	Zero liquid discharge

Nomenclature

Symbol	Unit	Description
Parameters (constant values, exogenously determined)		
C	–	Set of all desalination plant configurations in the study that can be regarded as mutually exclusive projects ($c \in C$).
$C^{larger\_projects}$	–	Set of all desalination plant configurations (or projects) larger than the smallest project c^{small}. In this study, the larger projects are 4P_1 and 4P_2 configurations.
c^{small}	–	The smallest of the mutually exclusive projects (2P_1 in this study).
$T^{mfa}(c)$	–	Set of technologies in a plant configuration c for which mass-flow-based-cost allocation is calculated ($T^{mfa}(c) \subseteq T^{all}(c)$). This is applicable to technologies that do not directly yield a marketable product.
$T^{tca}(c)$	–	Set of technologies in a plant configuration c for which total cost allocation is calculated ($T^{tca}(c) \subseteq T^{all}(c)$). This is applicable to technologies that produce, directly or indirectly, a single marketable product along with a brine discharge, wherever applicable.
$T^{mva}(c)$	–	Set of technologies in a plant configuration c for which market-value-based-cost allocation is calculated ($T^{mva}(c) \subseteq T^{all}(c)$). This is applicable to technologies that do yield, directly or indirectly, more than one marketable product, with at least one of them being a direct yield.
Variables (values determined endogenously within the model)		
$\boldsymbol{CapInv}_{j,t}(c)$	$\frac{USD_{2023,constant}}{year}$	Capital investment in a technology j in a year t (usually year 0) in a plant configuration c.
$\boldsymbol{COGS}_{j,t}(c)$	$\frac{USD_{2023,constant}}{year}$	Cost of goods sold (usually consisting of direct costs, like those for electricity and chemicals) for a technology j in a year t in a plant configuration c.
$\boldsymbol{cs}_j^{mfa}(p,c)$ or $\boldsymbol{cs}_j^{tca}(p,c)$ or $\boldsymbol{cs}_j^{mva}(p,c)$	–	Cost share of a technology j in the levelized cost of product p in a plant configuration c. The cost share allocation can be based on mass flow, total cost of the technology or market-value of the products.
$\boldsymbol{DALC}(p,c)$	$\frac{USD_{2023,constant}}{m^3 \text{ or } ton}$	Discounted and allocated levelized cost of a product p in a plant configuration c, represented in per m^3 or ton, if it is a water or mineral product, respectively.
$\boldsymbol{IRR}(c)$	–	Internal rate of return (IRR) of a plant configuration c.
$\boldsymbol{IRR}^{incremental}(c)$	–	Incremental internal rate of return (IRR) of a plant configuration c that is larger (and more expensive) than the configuration c^{small} (a mutually exclusive project) it is compared with.
$\boldsymbol{NPV}(c)$	$USD_{2023,constant}$	Net present value (NPV) of a plant configuration c.
$\boldsymbol{OtherCosts}_{j,t}(c)$	$\frac{USD_{2023,constant}}{year}$	Other costs (usually consisting of fixed and indirect costs) for a technology j in a year t in a plant configuration c.
$\boldsymbol{Revenue}_{j,t}(c)$	$\frac{USD_{2023,constant}}{year}$	Revenue resulting from the sale of product(s) produced by a technology j in a year t (usually begins from year 1) in a plant configuration c.
$\boldsymbol{Salvage}_{j,t}(c)$	$\frac{USD_{2023,constant}}{year}$	Salvage value related to the capital investment for a technology j in a year t (usually in the last year of its operation) in a plant configuration c.
$\boldsymbol{Tax}_{j,t}(c)$	$\frac{USD_{2023,constant}}{year}$	Tax paid based on the country's corporate tax for a technology j for any income (either from salvage or profits) in a year t in a plant configuration c.
$\boldsymbol{TPCF}_{j,t}(c)$ or $\boldsymbol{TPCF}_{j,t}^{wo\_revenue}(c)$	$\frac{USD_{2023,constant}}{year}$	Total project cash flow for a technology j in a year t in a plant configuration c. It can be calculated either with or without accounting for revenues from the products.
$\boldsymbol{TPCF}_{j,t}^{incremental}(c)$	$\frac{USD_{2023,constant}}{year}$	Total incremental project cash flow for a technology j in a year t in a plant configuration c that is larger (and more expensive) than the configuration c^{small} (a mutually exclusive project) it is compared with.

1. Introduction

The Middle East and North Africa (MENA) region is beset by a complex array of interconnected challenges, including severe water scarcity and food insecurity. Sixteen of the 25 countries under "extremely high water stress" (using over 80 % of renewable water

supply) are located in this region, impacting 83 % of its population [1]. Climate change-induced impacts are expected to further aggravate water scarcity [2], heightening competition among domestic, agricultural, and industrial sectors. Agriculture— the largest water consumer in countries like Morocco—is a critical source of food and income for the region [3]. However, the region continues to struggle with low food self-sufficiency rates, compromising its food security [4]. Paradoxically, the region—particularly the Gulf—hosts major export-oriented fertilizer industries, enabled by cheap natural gas [5]. While increasing domestic food production through fertilizers can help alleviate the region's food insufficiency, there are significant environmental drawbacks.

The production of synthetic fertilizers is energy- and water-intensive, and is responsible for a global greenhouse gas (GHG) emission of approximately 0.48 Gt of CO_2-equivalent [6,7]. For instance, the production of each ton of urea, a widely used nitrogen-based synthetic fertilizer, consumes up to 24 m^3 of freshwater and 887 standard cubic meters of natural gas, thereby releasing up to 0.76 tons of CO_2 into the atmosphere [7]. Conversely, studies have shown that decarbonization of fertilizer production through the use of renewable hydrogen and electricity is economically viable [7,8], offering a more sustainable solution. However, securing sufficient water supply for these operations remains a challenge. Seawater desalination can be an attractive solution to mitigate this issue, with the MENA region already accounting for nearly half of the global desalination capacity [9]. Given the export-oriented nature of the fertilizer production in this region, a strategic co-location of fertilizer and desalination plants near seaports presents an opportunity for resource optimization and circular economy principles. While such co-locations are emerging in the region [10], desalination is nevertheless accompanied by significant volumes of waste brine, over 142 million m^3 per day globally [9]. The traditional disposal techniques include surface water discharge, sewer discharge, and deep-well injection [11]. Brine disposal makes up 5–33 % of the total desalination costs, with actual costs depending on the characteristics and volume of the brine, the level of pretreatment, means of disposal and the nature of disposal environment [12]. Apart from the economic costs associated with conventional brine disposal, environmental concerns related to the brine's salinity, temperature, and chemical composition have been reported [11], although

Table 1
Comparison between proposed MLD scheme and other MLD/ZLD schemes from the literature.

Reference	Treatment chain/ technologies	Field/feedwater source	Region	Products	Mineral recovery	DCF-based levelized cost	Economic comparison of mutually exclusive projects
Al Bazedi et al. (2014) [19]	NF/RO-MCr/ evaporator/pond	Desalination	–	Freshwater, salt mixture (NaCl, $MgSO_4$)	✓	×	✓(simple rate of return)
Zhang et al. (2017) [20]	Precipitation, ED-BMED	Desalination	China	HCl, NaOH, NaCl	✓	× (simple)	×
Micari et al. (2019) [21]	NF-crystallizers-MED	Water softening plant	Netherlands	Concentrated brine as regenerant for IX, freshwater, Mg $(OH)_2$, $Ca(OH)_2$	✓	× (simple)	×
Ortiz-Albo et al. (2019) [17]	IX, adsorption, LLE, precipitation/ crystallization	Desalination	–	Minor elements (Li, Rb, In, Ba, Ni, U, Cs, Ge)	✓	×	×
Eiff et al. (2021) [22]	MSF-Cr	Desalination	–	Freshwater, $Na_2SO_4{\cdot}10H_2O$			
Pawar et al. (2022) [23]	NF-RO-ED-crystallizers	Coal mine	Poland	Freshwater, NaCl, Mg $(OH)_2$, $CaSO_4$	✓	× (simple)	×
Panagopoulos (2022) [11]	RO-BC-BCr/WAIV	Desalination	Eastern Mediterranean	Freshwater, solid salts	✓	× (simple)	✓(daily profits)
Morgante et al. (2022) [24]	NF-MRC-MED-NTC	Desalination	Italy	Freshwater, NaCl, Mg $(OH)_2$, $Ca(OH)_2$	✓	× (simple)	×
Del Villar et al. (2023) [18]	–	Desalination	Atlantic Ocean, Mediterranean Sea, brackish underground	Na, Mg, Ca, Sr, minor elements (Li, Rb, B, Ga)	✓	×	×
Sharkh et al. (2023) [13]	NF-SWRO-HPRO-OARO	Desalination	Saudi Arabia	Freshwater, NaCl brine	×	× (simple)	× (water recovery [%] & energy consumption only)
Abdalrhman et al. (2025) [25]	NF-SWRO-HPNF	Desalination	Saudi Arabia	Freshwater, NaCl brine	×	×	× (NaCl conc. & energy consumption only)
this paper	NF-SWRO-HPRO-OARO-crystallizers	Desalination for decarbonized fertilizer production	Morocco (Eastern Mediterranean)	Freshwater, UPW, NaCl, $Mg(OH)_2$	✓	✓ (own method)	✓(NPV and IRR)

Abbreviations not in acronyms table: BCr: brine crystallizer; BMED: bipolar membrane electrodialysis; ED: electrodialysis; HPNF: high-pressure nanofiltration; LLE: liquid-liquid extraction; MCr: membrane crystallizer; MED: multi-effect distillation; MRC: magnesium reactive crystallizer; MSF-Cr: multi-stage flash crystallizer; NTC: NaCl thermal crystallizer; WAIV: wind-aided intensified evaporation.

properly monitored and managed discharges are generally considered environmentally safe [13]. Addressing these interrelated challenges—water and food scarcities in the MENA region, along with the economic and environmental issues of brine disposal from seawater desalination—requires innovative solutions.

Using innovative brine management strategies, such as minimum liquid discharge (MLD) and zero liquid discharge (ZLD), can help tackle the brine disposal issue for desalination plants co-located with decarbonized fertilizer production facilities. While ZLD aims for a 100 % water recovery and an elimination of liquid waste through salt recovery, the MLD approach aims for lower recoveries (up to 95 %) at much lower costs and energy consumption [14].

1.1. Current state of knowledge

To the best of the authors' knowledge, no published study has examined MLD desalination specifically within the fertilizer industry. Existing literature has largely explored the techno-economic feasibility of decarbonized production—such as ammonia and urea [7,8, 15]—without integrating MLD desalination. For example, a prior work [7] assessed several decarbonization pathways for Indian urea plants were analyzed and demonstrated that producing "green" urea—produced using renewable hydrogen and captured CO_2—could achieve economic feasibility and reduce water consumption by 40 %.

MLD/ZLD in desalination - Focus areas and elements recovered: Most studies on MLD and ZLD approaches in seawater desalination focus on technical and techno-economic analyses (TEA) for mineral recovery from brines outside the fertilizer sector. Table 1 overviews these studies, which primarily evaluate treatment chains aiming to maximize brine valorization and enhance economic viability by co-recovering minerals—typically magnesium and sodium chloride, due to their abundance and favorable economics [16]. While a few works have considered the extraction of minor elements (e.g., lithium, rubidium, indium, uranium), their

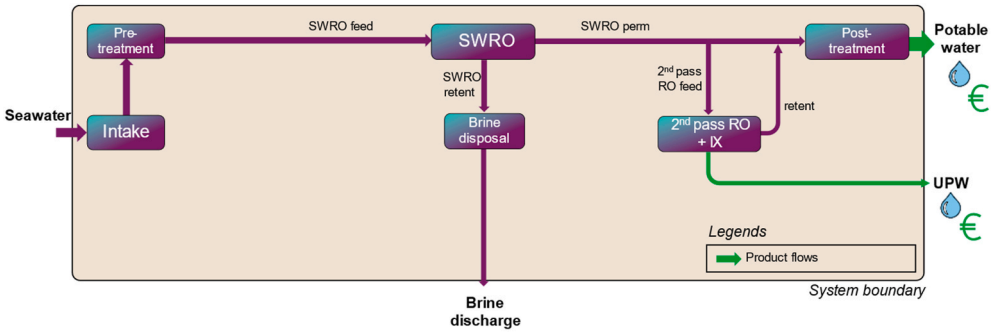

(a) Conventional desalination configuration (2P_1)

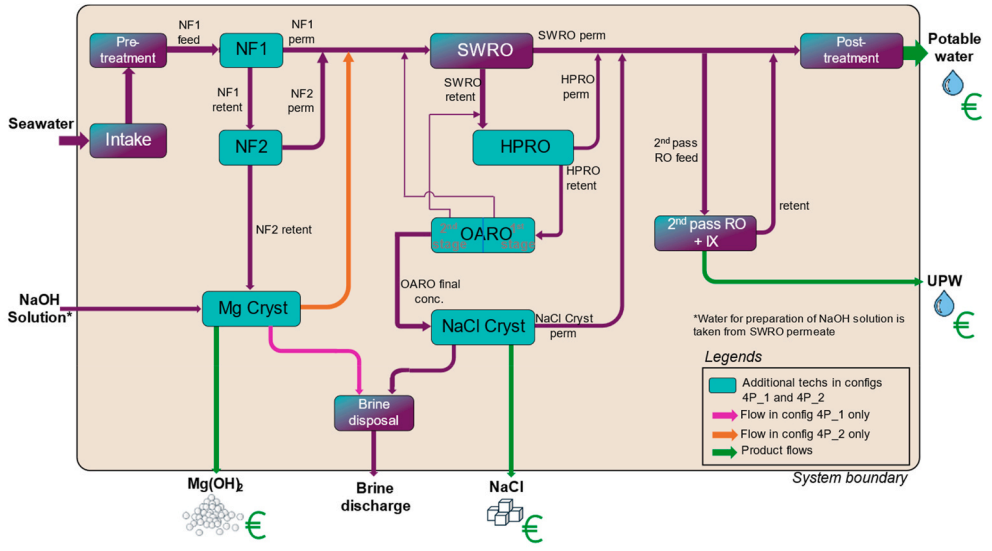

(b) MLD configurations (4P_1 and 4P_2)

Fig. 1. Process-flow diagram (PFD) showing material flows of the three desalination plant configurations: (a) conventional desalination configuration (2P_1); (b) MLD configurations (4P_1 and 4P_2).

large-scale recovery faces technical and economic barriers related to low concentrations and limited technology readiness [16–18].

Salt and mineral recovery studies: Numerous TEAs have assessed salt and mineral recovery chains involving combinations of evaporation ponds, membrane crystallizers, and brine concentrators (BC). Al Bazedi et al. (2014) reported that salt recovery using membrane crystallizers could significantly improve desalination economics, achieving high returns at large scales [19]. Similarly, Zhang et al. (2017) demonstrated that recovering NaOH and HCl form seawater RO concentrate via electrodialysis could be cost-competitive [20]. Other studies examined valorization of specific products—such as Glauber's salt [22], regenerant solutions for ion-exchange (IX) resins [21], $CaSO_4$, $Ca(OH)_2$, $Mg(OH)_2$ and NaCl [23,24]—with outcomes ranging from economically viable to unattractive (e.g., high NaCl recovery costs from coal mine effluents [23]). Across these examples, high energy demand and chemical input often represent major operational cost drivers.

System-level and comparative analyses: A few works have evaluated complete ZLD treatment chains. Panagopoulos (2022) evaluated RO–BC-crystallizer combinations and estimated modest daily profits [11]. Morgante et al. (2022) combined NF, reactive crystallization, reporting that substantial $Mg(OH)_2$ revenue could offset high operating costs, allowing the system to breakthrough [24]. Sharkh et al. (2023) piloted a dual brine concentration concept that separates monovalent and divalent ions using high-pressure RO (HPRO) and a two-stage osmotically assisted RO (OARO) as a membrane brine concentration (MBC) system, improving raw material supply potential for downstream industries, though their economic analysis did not extend to mineral recovery steps [13]. Building upon this work, the authors' recent publication [25] presents novel NF membranes with higher Ca and Mg rejections at a high permeate recovery, along with a 3-stage high pressure NF (HPNF) as their MBC system, thereby achieving significantly higher NaCl concentration (230 vs. 168.4–176.6 g/L [13]). However, extending such treatment chains with additional crystallization or reactive steps can improve their overall financial analysis.

Financial modeling approaches: Most TEAs in the literature use simplified levelized cost (LC) calculations, discounting only capital costs via a capacity recovery factor or CRF while leaving operational costs undiscounted [26]. This yields conservative results [21] and neglects important financial aspects such as taxation and depreciation. For multi-product systems, LC often assigns revenues from co-products to the main product, risking skewed cost analysis and overly optimistic revenue assumptions. Some studies used non-standard indicators (e.g., daily profits [11], maximum initial investment [17], simple rate of return [19]), complicating cross-comparison. Furthermore, few studies compare alternative treatment chains directly using standard financial metrics such as net present value (NPV) or internal rate of return (IRR).

Industrial applications and integration gaps: Industrial applications of MLD/ZLD remain limited, with only a few examples: treating coal mine effluents [23] or regenerant recovery for IX resins [21]. For "green" ammonia production—produced using renewable hydrogen—several studies considered seawater desalination using seawater reverse osmosis (SWRO) or thermal methods (e.g., multi-effect distillation (MED), mechanical vapor recompression (MVR)) [27–30], but none have analyzed the technology chain for ultrapure water (UPW) production—a key requirement for electrolytic hydrogen—or explored MLD/ZLD integration with seawater desalination for decarbonized fertilizer manufacturing. This presents a knowledge gap addressed in the present study.

1.2. Objective and research questions

This study addresses the identified research gaps by conducting a TEA of seawater desalination designed for fertilizer production needs, comparing three configurations (Fig. 1): (i) a conventional setup (2P_1) producing only freshwater and UPW without MLD/ZLD, (ii) a base MLD configuration (4P_1) that additionally recovers $Mg(OH)_2$ and NaCl through NF, HPRO, OARO, and crystallizers, while discharging magnesium crystallizer effluent; and (iii) an enhanced MLD configuration (4P_2) that reuses the magnesium crystallizer effluent to maximize brine utilization.

1.3. The study aims to answer three research questions

1. **Environmental impacts:** What are the benefits (water and mineral recovery, brine minimization) and trade-offs (higher specific electricity consumption or SEC) of base and maximized MLD configurations relative to conventional desalination?
2. **Economic viability:** How do MLD strategies affect production costs—assessed via conventional LC and a novel Discounted and Allocated Levelized Cost, DALC— and financial performance (NPV, IRR)?
3. **Sensitivity:** How does financial viability respond to changes in discount rate, electricity price, and mineral costs, and what measures can enhance the performance of maximized MLD configuration relative to the base MLD?

Table 2
Ion concentration of major ions in the Eastern Mediterranean Sea vs. reference seawater [31].

Sea	Ion Species [mg/L]						TDS [mg/L]
	Cl^-	Na^+	SO_4^{2-}	Mg^{2+}	Ca^{2+}	HCO_3^-	
Eastern Mediterranean	21,200	11,800	2950	1403	423	–	38,600
Reference seawater	18,980	10,556	2649	1262	400	140	34,483

2. Methods

This chapter outlines the case study, the three desalination configurations under assessment, and the TEA approach, including evaluation indicators and sensitivity analyses.

2.1. Case study design

The case considers a hypothetical decarbonized urea production facility on Morocco's Mediterranean coast, chosen for its proximity to the European market and seawater with above-average ion concentrations (~12 % higher total dissolved solids (TDS) than reference seawater, Table 2), offering enhanced mineral recovery potential. Bicarbonate data were unavailable and excluded.

As a fertilizer reference plant, the highly efficient HURL Sindri plant (India, 1.27 $Mt_{urea}/year$) was chosen [7]. The water and "green" hydrogen—from renewables—requirements for its decarbonized version [7] defined the desalination plant's intake flow. For an hourly urea production of 160.35 t_{urea}/h (330 days/year), potable water and green H_2 needs are 4 $m^3_{potable\_water}/t_{urea}$ (or 641.4 $m^3_{potable\_water}/h$) and 0.1 t_{H2}/t_{urea} (or 16.035 t_{H2}/h), respectively. Based on the electrolyzer's UPW demand of 10 $m^3_{UPW}/\ t_{H2}$ [32] and a 75 % recovery UPW rate from potable water [33], the hourly UPW demand is 160.35 m^3_{UPW}/h, needing 213.8 $m^3_{potable\_water}/h$. The total hourly potable water requirement (641.4 + 213.8) was rounded up to 1000 $m^3_{potable\_water}/h$. While a conventional design could meet the water demand, MLD options were explored to reduce brine discharge and enable mineral recovery.

2.2. Overview of the three treatment chain configurations

Conventional configuration (2P_1, Fig. 1 (a))

The conventional setup ("2P_1": two main products, variant 1) includes seawater intake, pretreatment, a SWRO unit, second-pass RO with IX, post-treatment, and brine disposal. Following pretreatment (coagulation-flocculation-media filtration) [34], SWRO was selected for its energy efficiency and market dominance [35]. To produce UPW (TDS <0.5 ppm) for electrolysis, part of the SWRO permeate was processed by a second-pass RO followed by an IX unit [36]. The SWRO retentate (approximately 40 % of SWRO feed), without mineral recovery, was discharged as brine into the ocean via surface water discharge. Two MLD-based configurations were developed to address this.

Base MLD configuration (4P_1, Fig. 1 (b))

The 4P_1 configuration reduces brine discharge and recovers two additional products: $Mg(OH)_2$ and NaCl. As shown in Fig. 1 (b), additional technologies (inspired by SWCC's NF-RO-MBC pilot plant [13]) are incorporated. Pretreated seawater—rich in scale-forming bivalent ions—is first processed by NF, which removes 60–99 % of bivalent ions (e.g., Mg^{2+}, Ca^{2+}, SO_4^{2-}) [24]. This reduces membrane fouling, lowers downstream osmotic pressure, improves water recovery (up to 30 %), and decreases energy use [13,24,37,38]. The NF retentate is further concentrated, supporting enhanced $Mg(OH)_2$ recovery, while also enhancing the recovery of monovalent-ion-rich permeate for potable water and NaCl production. While the bivalent stream contained additional ions (Ca^{2+}, SO_4^{2-}, etc.), $Mg(OH)_2$ recovery was prioritized due its significantly higher concentration in seawater—typically about five times greater than calcium—and its higher market value [16]. Magnesium recovery was carried out in a reactive crystallizer, where $Mg(OH)_2$

Table 3
Key flow parameters for 4P_1 configuration (Eastern Mediterranean Sea).

Technology	Trains	Stream	Pressure [bar (g)]	Flow [m3/h]	TDS [ppm]	Notes
NF1	5	Feed	28.0	2000.0	37,417	–
		Permeate	0.0	999.1	24,215	–
NF2	5	Feed	50.0	1020.0	49,324	–
		Permeate	0.0	513.1	31,000	–
Magnesium crystallizer	3	Feed	0.0	518.9	62,649	–
		Effluent	0.0	573.1[b]	61,630	Includes NaOH addition
SWRO	3	Feed	72.4	1516.2	24,741.4[c]	After mixing the OARO dilute (1st stage)
		Permeate	1.0	1027.6	205[c]	–
HPRO	3	Feed	113	1020.5[d]	72,148[d]	After mixing the OARO dilute (2nd stage)
		Permeate	1.0	255.3	550	–
OARO (1st stage)	3	Feed	70.0	1194.8[d]	97,891[d]	–
		Dilute	0.0	533.27	70,463	–
OARO (2nd stage)	3	Feed	69.0	661.8	119,234	–
		Dilute	0.0	429.6	100,704	–
		Final concentrate	0.0	233.5	158,734[e]	Assumes 176,600 mg/L and density 1.1125 kg/L
NaCl crystallizer	3	Feed	0.0	236.1	158,734 or 146,761 of NaCl	–
		Permeate	0.0	212.7	<10	–
2nd pass RO + IX	2	Feed	–	213.8	205	–
		Permeate	0.0	160.3	<0.5	UPW

was precipitated by adding an alkaline solution, specifically, NaOH. The addition of NaOH supplies hydroxide ions (OH^-), which react with dissolved Mg^{2+} ions to form solid $Mg(OH)_2$. Simultaneously, the resulting increase in pH (to approximately 9.5–10) reduces the solubility of magnesium, thereby promoting efficient and selective precipitation of $Mg(OH)_2$ [39]. The water required for the NaOH solution was sourced internally by diverting a portion of the produced SWRO permeate. The NF permeate was fed to the SWRO unit, generating permeate and retentate of a quality comparable to that in configuration 2P_1. However, instead of being discharged as a brine, the monovalent-ion-rich SWRO retentate in 4P_1 was used for NaCl recovery. To limit the size of the downstream cost- and energy-intensive NaCl crystallizer based on mechanical vapor recompression (MVR), the SWRO retentate was concentrated beforehand using two energy-efficient membrane technologies: a HPRO unit (to a concentration of around 110,000 ppm) and then a two-stage OARO system (to a concentration of around 158,700 ppm) [13]. The HPRO unit also produced a high-quality permeate of around 550 ppm. The OARO generated two low-salinity dilute streams that were recirculated: the first-stage dilute (around 70,500 ppm) was fed to the HPRO, and second-stage dilute (around 100,700 ppm) was fed back to the first stage. The final concentrate from the OARO was processed by the MVR-based NaCl crystallizer, yielding high purity salt (99.8 %) and distilled water. The purge stream from the salt crystallizer, along with the magnesium crystallizer effluent, were discharged into the sea. The substantial effluent volume from the magnesium crystallizer (see Table 3) meant that a significant brine discharge reduction compared to the conventional plant (2P_1) was not achieved with configuration 4P_1, motivating the development of a third configuration (4P_2).

Maximized MLD configuration (4P_2, Fig. 1 (b))

In 4P_2, the magnesium crystallizer effluent is recycled to the SWRO feed instead of being discharged, maximizing water recovery from SWRO, HPRO and the NaCl crystallizer, and potentially improving the financial viability relative to 4P_1.

For all three configurations, the intake feed volume was set at 2000 $m^3_{feed\_intake}/h$ based on simulations meeting potable water and UPW demands for 4P_1—the most restrictive, due to internal water consumption and lack of crystallizer effluent recycling. Key flow parameters for 4P_1 appear in Table 3; all others are available under Data availability. Given that the flow rates in this study were approximately half of those in the commercial plant design proposed by Sharkh et al. (2023) [13], the chosen number of trains was correspondingly halved.

2.3. Technology overview

This subsection briefly discusses the overarching operating principles and techno-economic modeling of the desalination and brine concentration technologies employed to model the three desalination configurations. A more detailed explanation, along with the equations and values for key parameters, can be found in Appendix A.

- **Nanofiltration (NF):** NF is a pressure-driven membrane technology whose unique membrane property—lying between those of RO and Ultrafiltration (UF) —have propelled its application as a pretreatment technology in desalination plants for the removal of scale-forming bivalent ions. NF was modeled with a hierarchical structure comprising a low-, medium-, and high-hierarchy model [40]. The low-hierarchy model describes the transport mechanisms within the NF membrane using a Donnan Steric Pore Model with Dielectric Exclusion (DSPM-DE), which is based on the extended Nernst-Plank equation that considers a combination of three ionic transport mechanisms: (i) convection, (ii) diffusion, and (iii) electro-migration. Based on this, the medium-hierarchy model then described the NF element and was composed of mass and energy balance equations [40]. Finally, the high-hierarchy model regarded the whole NF plant and computed the total number of vessels to reach a certain recovery using an iterative approach. These results were then used in the economic model based on the Verberne cost model [41], allowing the calculation of (i) building cost for the plant housing, (ii) cost of pumps, filters and piping system, (iii) cost for the energy supply system, and (iv) membrane cost.
- **Seawater reverse osmosis (SWRO):** SWRO is a pressure-driven membrane process and a widely used technology for seawater desalination. The technology was modeled with a hierarchical structure comprising three levels. The low-hierarchy model described the transfer mechanisms of salt and water within the RO membrane using a two-parameter solution-diffusion model. The medium-hierarchy model then defined the RO unit by estimating the flow rate, concentration, and pressure profile using mass-balance equations. Finally, the high-hierarchy model regarded the whole RO plant and computed the total number of vessels per stage by determining the feed pressure using an optimization technique. These results were input to an economic model, which estimated the costs of membrane units, pressure vessels, pumps and piping.
- **Magnesium reactive crystallizer:** This crystallizer was modeled using simple mass-balance equations and used an alkaline reactant (NaOH solution) to promote precipitation of $Mg(OH)_2$. Stoichiometrically, each magnesium ion in the brine requires two hydroxyl ions from the reactant for precipitation. Given that the chemical reaction for $Mg(OH)_2$ precipitation occurs at a pH value of 10.35 [24], the effluent pH was elevated and subsequently neutralized to pH 6.5 using a 1M HCl solution.
- **HPRO and OARO**: The techno-economic modeling of these brine-concentration technologies was based on a simplified parametrization of performance metrics from Sharkh et al. (2023) [13], given the similarity in feed flow rates (2000 vs 4195 m^3/h). This simplification was made by constraining peripheral ion concentrations to match those in Sharkh et al. (2023). For instance, the SWRO retentate concentration was maintained at 74,000 ppm, consistent with their assumptions.
- **NaCl Crystallizer:** The salt crystallizer aimed to extract NaCl and distillate from the high-salinity OARO concentrate. The crystallizer consists of three sub-technologies: an evaporator, a de-watering unit, and a dryer for salt production [42]. While evaporators—being the most energy- and cost-intensive component— can be either steam-driven (multi-effect) or electrically driven (mechanical vapor recompression or MVR) systems, the electric option was selected due to its location-independent operability.

The techno-economic modeling of this crystallizer used a generic MVR-based commercial NaCl crystallizer costing 15 million USD_{2019} as a reference, producing 100,000 tons of salt annually with 150 kWh_{el}/ton_{NaCl} energy consumption [42]. The reference assumes a nearly saturated brine feed (250 $\frac{g_{NaCl}}{kg_{brine}}$) and 8 $\frac{g_{impurities}}{L_{brine}}$, with a purge ratio of 20 % to achieve 99.8 % salt purity. Based on actual feed concentration, the purge ratio was adjusted to compute the effective purge ratio. Changes in specific costs (capital and operating), and SEC from the reference system due to variations in feed salt concentration were captured by the crystallizer salinity scale-up factor (CSSF) [42]. A CSSF of 1.50, for example, indicates 50 % higher costs and energy usage than the reference.

- **Intake system:** The intake system of a seawater desalination plant includes structures (e.g., towers and wells), pipelines, and pumping stations equipped with coarse and fine screens [43]. Due to site-specific variability, a typical construction cost range of 90–120 $USD_{2018}/\left(m^3_{perm}/day\right)$ was used [43].
- **Pre-treatment:** Effective seawater pretreatment is crucial for membrane-based desalination plants. Foulants compounds can severely impede performance by blocking pores, leading to accelerated fouling and premature membrane replacement [43]. While both conventional (coagulation-flocculation-media filtration) and membrane-based (microfiltration, ultrafiltration) pre-treatment exist, the conventional method remains the most prevalent approach [34], and was selected in this study.
- **Post-treatment:** Post-treatment involves two main conditioning steps: stabilization to adjust its chemical balance (e.g., alkalinity and hardness) and disinfection [43]. The selected stabilization method uses lime ($Ca(OH)_2$) and CO_2. Disinfection was performed using sodium hypochlorite, similar to Sharkh et al. (2023) [13].

2.4. Financial modeling

This section summarizes the financial parameters and briefly discusses the indicators used for the financial analysis in this study (DALC, NPV or IRR). A detailed formulation of the three financial indicators is provided in Appendix B. All indicators were based on DCF analysis, a valuation method that estimates project value by summing all future cash flows over the project lifetime after discounting them to present value. The total project cash flows (TPCF) included components such as operating cash flows (OCF) and cost of goods sold (COGS), which were calculated using standard corporate finance practices [44] (see Appendix B.1). The discount rate, defined as the weighted average cost of capital (WACC), incorporated a technology-specific risk premium for MLD configurations to reflect the added complexity and lower technology readiness level (TRL) of certain MLD technologies (Appendix B.2).

The DALC metric (refer Appendix B.3 for its detailed derivation) was developed to individually allocate capital and operating expenditures of each technology to each product for a given configuration. It integrates multiple cost allocation strategies, including mass- and value-based allocations, while explicitly excluding revenue offsets from co-products in order to isolate cost-side burden of each product (see Equation (1)). This distinguishes DALC from conventional LC metrics, which typically net off revenues and obscures technology-cost distribution in multi-product systems.

$$\boldsymbol{DALC}(p,c)=\sum_{j}^{J}\frac{\sum_{t=0}^{t=n}\frac{\boldsymbol{TPCF}_{j,t}^{wo\_revenue}(c)}{(1+i(c))^t}}{\sum_{t=0}^{t=n}\frac{\boldsymbol{Q}_t(p,c)}{(1+i(c))^t}}\times \boldsymbol{cs}_j(p,c)\ \text{if}\ j\in T^{mfa},\boldsymbol{cs}_j(p,c)=\boldsymbol{cs}_j^{mfa}(p,c)\text{if}\ j\in T^{tca},\boldsymbol{cs}_j(p,c)=\boldsymbol{cs}_j^{tca}(p,c)\ \forall\text{cif}\ j\in T^{mva},\boldsymbol{cs}_j(p,c)$$

$$=\boldsymbol{cs}_j^{mva}(p,c)$$

Equation 1

The DALC equation for product p and configuration c depicts: (i) $\boldsymbol{TPCF}_{j,t}^{wo\_revenue}$ for a technology j and a project year t that excludes any revenue from the products; (ii) $\boldsymbol{Q}_t$ is the annual production amount of the product; and (iii) $\boldsymbol{cs}_j$ is the technology cost share based on one of the three cost allocation techniques, namely mass-flow-based cost allocation, total cost allocation, and market-value-based cost allocation.

NPV and IRR values for the 2P_1 configuration were calculated using the standard DCF methodology (Equation (2) and Equation (3), respectively. Refer Appendix B.4 for further details). As seen in these equations, NPV and IRR indicators are formally equivalent, theoretically allowing an interchangeable usage. However, when comparing mutually exclusive projects (such as the three configurations in this study), the use of IRR can lead to misleading results and incorrect project rankings [44]. To rectify this shortcoming of the IRR rule, an incremental flow method is applied, which requires the IRR for the smaller project (configuration 2P_1 in this study) be calculated using the standard methodology (Equation (3)), whereas those for the larger projects (configurations 4P_1 and 4P_2) be calculated incrementally in relation to the smaller project (Equation (4) and Equation (5)) [44]. The NPV for the larger projects is calculated using the standard methodology (Equation (2)).

$$\boldsymbol{NPV}(c)=\sum_{j}^{J}\sum_{t=0}^{t=n}\frac{\boldsymbol{TPCF}_{j,t}(c)}{(1+i(c))^t}\ \text{if}\ c=c^{small}$$

Equation 2

$$\sum_{j}^{J}\sum_{t=0}^{t=n}\frac{\boldsymbol{TPCF}_{j,t}(c)}{(1+\boldsymbol{IRR}(c))^t}=0\ \text{if}\ c=c^{small}$$

Equation 3

$$\boldsymbol{TPCF}_{j,t}^{incremental}(c)=\boldsymbol{TPCF}_{j,t}\left(c^{large}\right)-\boldsymbol{TPCF}_{j,t}\left(c^{small}\right)\ \text{if}\ c\in C^{larger\_projects},\forall j,\forall t$$

Equation 4

$$\sum_{j}^{J}\sum_{t=0}^{t=n}\frac{\boldsymbol{TPCF}_{j,t}^{incremental}(c)}{\left(1+\boldsymbol{IRR}^{incremental}(c)\right)^{t}}=0 \text{ if } c\in C^{larger\_projects} \quad \text{Equation 5}$$

Assumptions for key financial parameters are summarized in Table 4. All monetary values are expressed in "real" or constant 2024 US dollars, with literature values adjusted using CEPCI (chemical engineering plant cost index).

2.5. Sensitivity analysis

To identify key financial drivers for MLD configurations relative to conventional desalination, sensitivity analysis was performed on 4P_1 and 4P_2. Six mutually independent parameters were varied: capital investment, revenue, COGS, other costs, discount rate, and risk premium. Depreciation and salvage value were excluded, as they depend directly on capital investment. Each parameter was varied independently by ±50 % of its base value, with NPV chosen as the sole indicator since it captures all six parameters.

Although 4P_2 maximizes brine minimization through effluent reuse, Section 3.5 show it underperforms 4P_1 in IRR and NPV. To evaluate conditions for financial parity:

1. **Brine discharge levy on 4P_1**: Brine disposal cost (BDC) was incrementally raised, simulating an environmental effluent charge, until IRR and NPV matched those of 4P_2.
2. **Preferential financing for 4P_2:** The WACC was progressively reduced, simulating a policy-backed financing incentive, until IRR and NPV matched those of 4P_1.

3. Results and discussion

This section first presents the technical results (flow rates and SEC) across the three configurations, followed by the financial results (conventional LC, DALC, NPV and IRR, and sensitivity analysis).

3.1. Flow rate comparison: reduction in brine disposal using MLD is not a given

Fig. 2 (a) and 2 (b) present the key water (m^3/h) and material (ton/h) flow rates, respectively. UPW demand was exogenously fixed by the fertilizer plant's hydrogen needs and remained identical across all cases. Other flows—potable water, brine, and minerals—were determined endogenously.

In 4P_1, brine discharge was reduced by only 22.7 % compared to 2P_1, due to direct discharge of magnesium crystallizer effluent. Total water recovery only modestly improved (71.4 % vs. 60.4 %).

In 4P_2, recycling the magnesium crystallizer to SWRO boosted this recovery to 96.7 %. While 4P_2's brine discharge reduced by 88 % as compared to 2P_1, its potable water recovery rose by only 69 %, as a result of a sixfold increase in NaCl crystallizer purge volume relative to 4P_1 (driven by higher feed impurities: 14.9 vs 4.0 $\frac{g_{impurities}}{L_{brine}}$), resulting from the upstream blending of the magnesium crystallizer effluent. To maintain NaCl purity, the purge ratio had to be raised (21.3 % vs 5.8 % in 4P_1). Despite this, the NaCl recovery increased by ~18 % due to higher feed flow, while $Mg(OH)_2$ recovery and NaOH consumption remained unchanged across both MLD cases.

Table 4
Key financial assumptions for TEA (constant 2024 USD).

Category	Parameter	Value/Assumption
General	Currency base	USD (2024, constant)
	Cost adjustment	CEPCI indices
	Conversion rate	9.89 MAD/USD (Feb. 2025)
	Plant availability	96 % [13]
Discounting	Real discount rate (2P_1)	7 %
	Real discount rate (4P_1, 4P_2)	8.75 % (incl. +25 % risk premium)
Corporate finance	Corporate tax	20 % (for net taxable income <100M MAD) [45]
	Depreciation	Declining balance, 12.5 % (avg. 10–15 % [45])
	Salvage value	5 % of capital investment [46]
Energy and O&M	Electricity price (renewable)	0.07 USD/kWh_{el} (PV systems 0.06–0.08 USD/kWh_{el} [47])
	Labor – operator	16,784 USD/a (166,000 MAD/a [48])
	Labor – chemist	21,819 USD/a (1.3x operator [42])
	Labor – engineer	26,854 USD/a (1.6x operator [42])
Brine management	Disposal cost (BDC)	0.04 USD/m^3 [12]
Key commodities	NaOH	350 USD/t [24]
	HCl	150 USD/t [24]
Products	Potable water	1.5 USD/m^3 [49]
	UPW	2.5 USD/m^3 [50]
	$Mg(OH)_2$	1000 USD/t [24]
	NaCl	80 USD/t [42]

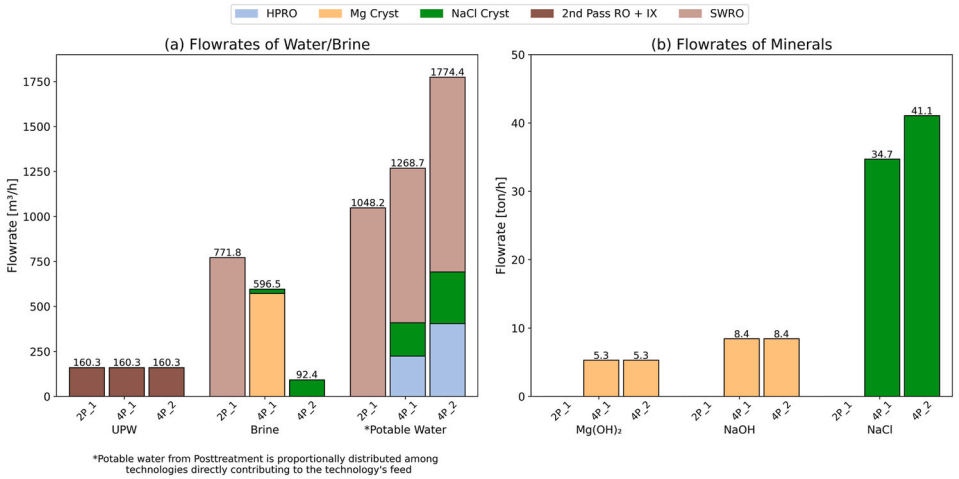

Fig. 2. Material flow rate diagrams for the three desalination configurations. (a): flow rate of water and brine in m^3/h. (b): flow rate of input (NaOH) and output ($Mg(OH)_2$, NaCl) minerals in ton/h.

In short, in terms of water recovery and brine minimization, 4P_1 offers only marginal improvements over conventional 2P_1, whereas 4P_2 achieves substantial improvements but at the expense of increased NaCl crystallizer efficiency and process complexity.

3.2. SEC comparison: NaCl crystallizer dominates in MLD

Fig. 3(a–c) shows SEC distribution for 2P_1, 4P_1, and 4P_2, respectively, while Fig. 3 (d) compares their total SEC. Normalized to

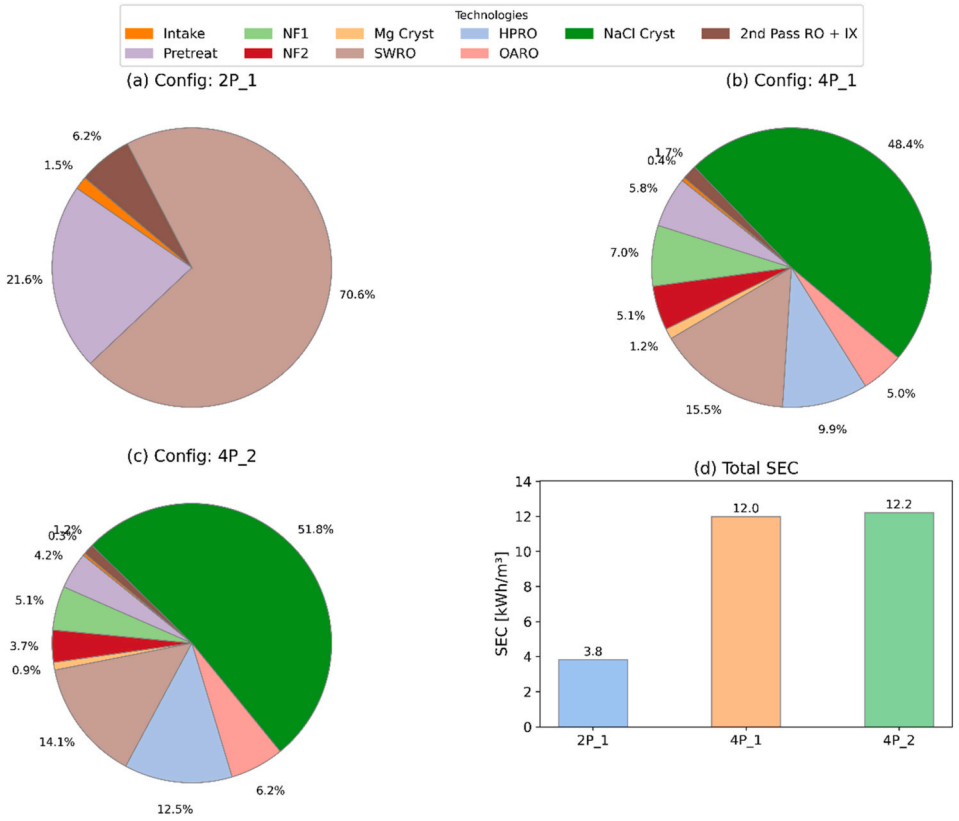

Fig. 3. SEC comparing the three desalination configurations. The SEC share per technology is shown as pie chart, whereas total value (in $kWh_{el}/\ m^3$ of potable water + UPW) is shown in the bar chart.

the feed, the total SECs were 2.3, 8.6, and 11.8 kWh_{el}/m^3_{feed}, respectively—up to 3.2 times higher for the MLD cases.

In 4P_1, the NaCl crystallizer accounted for 48 % of total SEC, with a salt-specific SEC of 238 kWh_{el}/t_{NaCl}, 59 % above the commercial benchmark (150 kWh_{el}/t_{NaCl} [42]). The excess is explained by the relatively dilute feed (146.7 vs. 250 $g_{NaCl}/\ kg_{sol}$ in industrial settings).

In 4P_2, the per-water SEC of the NaCl crystallizer was 15 % lower than in 4P_1 (29.7 vs 35.1 kWh_{el}/m^3) due to higher water output (see Fig. 2). However, its per-salt SEC increased by 25 %–297 kWh_{el}/t_{NaCl}, due to higher feed impurity load and associated purge requirements.

By contrast, in 2P_1, SWRO dominated the SEC (>70 %), followed by pretreatment (21.6 %). In MLD configurations, SWRO's share dropped to 15 % (4P_1) and 14 % (4P_2), while HPRO contributed 10–12.5 %. All other technologies in MLD setups contributed ≤7 %.

In summary, MLD configurations are substantially more energy-intensive, than conventional desalination, with performance dominated by the NaCl crystallizer. Feed salinity and impurity content, determined by upstream process integration, are key levers for NaCl crystallizer efficiency.

3.3. DCF components: taxes are a non-negligible outflow often ignored in LC calculations

Examining the core DCF components (Fig. 4; terminology and equations in Appendix B.1) helps contextualize the financial indicators DALC, NPV, and IRR. The figure shows revenues, variable and fixed costs, capital expenditures, taxes, and depreciation, while excluding aggregate terms like pretax profit and TPCF. Depreciation, though a non-cash item, was included because it shapes taxable income and thereby tax-related cash flows (Equation B-2).

The cash flow profiles differed markedly across configurations. The conventional 2P_1 showed the narrowest spread—about six times smaller than 4P_2, the most capital- and energy-intensive setup. This wider spread in MLD schemes reflects not only higher investments and operating costs, but also the substantial revenues from mineral recovery. Cumulative revenues in 4P_1 and 4P_2 were 4.5 and 5.1 times higher, respectively, than in 2P_1.

Cost distribution also varied across cases. In 2P_1, capital investment and taxes each contributed roughly 27 % of total outflows. In the MLD cases, variable costs (captured by *COGS*, mainly NaOH costs for magnesium crystallization) dominated, reaching 38 % of outflows. Taxes and depreciation consistently outweighed fixed costs (denoted as *otherCosts*) with taxes alone ranging from 13 to 27 % of the total outflow, depending on configuration.

Overall, the results highlight that taxes and depreciation are significant financial drivers. Their omission or oversimplification—as is common in conventional LC approaches (e.g., ignoring taxes or assuming straight-line depreciation via CRF)—can bias LC-based cost estimates and understate project risks.

3.4. DALC vs conventional LC: lower DALC for conventional desalination; mixed outcomes for MLD configurations

The main differences between DALC and conventional LC lie in cost allocation, the time value of money, and the treatment of co-product revenues. DALC applies full DCF at the technology level and excludes revenues, while conventional LC discounts only capital costs, spreads operating costs uniformly, and subtracts co-product revenues. As a result, DALC offers more granular breakdown, whereas conventional LC can yield lower—or even negative—costs when revenues are substantial. Fig. 5 illustrates these contrasts, showing DALC as stacked bars and conventional LC as scatter points.

For water, DALCs in the conventional configuration (2P_1) were up to 47 % and 93 % lower for potable water and UPW, respectively, than in MLD cases. Between MLD setups, 4P_2 showed higher water DALCs than 4P_1, owing to additional cost allocation from the magnesium crystallizer (which contributed to water recovery) and higher NaCl crystallizer costs resulting from a higher CSSF

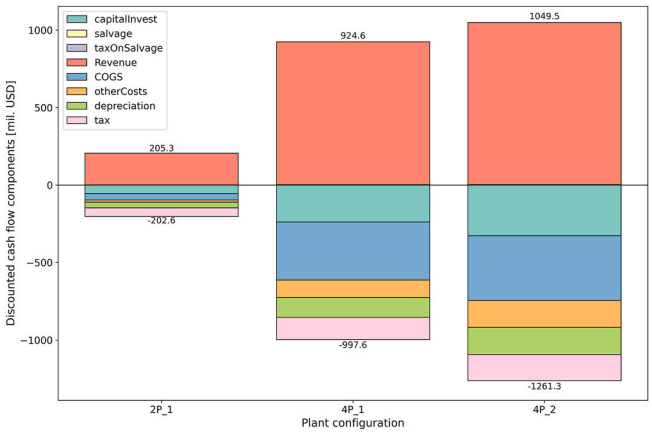

Fig. 4. DCF components (only the fundamental ones) for the three desalination configurations. Except revenue, the remaining components are shown as cash outflows (negative y-axis).

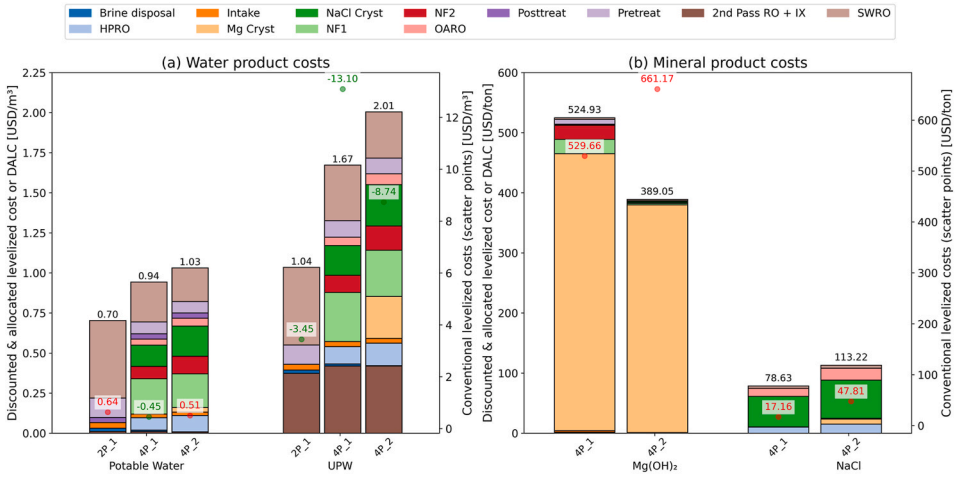

Fig. 5. DALC (stacked bar plots, primary y-axis) along with conventional LC (scatter plots, secondary y-axis) for the three desalination configurations: (a) water products, and (b) mineral products. Negative conventional LC indicates a net income (green), positive LC is net outflow (red).

(crystallizer salinity scale-up factor) due to increased impurities and purge ratio (Appendix A.5).

For minerals, the $Mg(OH)_2$ DALC in 4P_2 was 35 % lower than in 4P_1, since part of its costs were redistributed downstream through effluent reuse. In contrast, the NaCl DALC in 4P_2 was 44 % higher, driven by the increased CSSF of the NaCl crystallizer and greater cost shares from HPRO and OARO due to the handling of larger brine volumes.

Conventional LCs showed mixed outcomes. Mineral LCs in 4P_2 were markedly higher than in 4P_1–179 % for NaCl and 25 % for $Mg(OH)_2$—because HPRO and OARO costs rose by 43 % and NaCl crystallizer costs by 34 %, without offsetting revenue gains. For water, 4P_2 underperformed 4P_1: UPW revenues were lower, and potable water incurred a cost of 0.51 USD/m^3 compared with a revenue of 0.45 USD/m^3 in 4P_1. Nevertheless, 4P_2 still slightly outperformed 2P_1 in water costs.

In summary, 2P_1 and 4P_2 yielded the lowest and highest water DALCs, respectively, with the latter penalized by effluent reuse. By contrast, conventional LC—because it incorporates co-product revenues—tended to favor 4P_1. Ultimately, while DALC clarified product-level technology cost burdens, investment choices among configurations were more strongly guided by NPV and IRR results.

3.5. *NPV and IRR comparisons: diminishing rate of return with higher mineral recovery*

Fig. 6 presents NPVs and IRRs for the three configurations. NPVs are shown as stacked bars by technology (primary y-axis), with totals as red scatter plots (secondary y-axis). IRRs are displayed as blue scatter plots (tertiary y-axis), with incremental IRRs for the MLD cases.

In the conventional configuration (2P_1), SWRO generated the largest net cost (82 % of NPV), while post-treatment supplied the main net income (177 %) through potable water sales. UPW production via second-pass RO + IX added another 35 % to NPV. Together, these yielded a total NPV of ~72.1 million USD and the highest IRR (~24 %).

The base MLD configuration (4P_1) nearly doubled the NPV to 137.7 million USD. The $Mg(OH)_2$ and NaCl crystallizers contributed most to net income (112 % and 32 %), while OARO and SWRO imposed the largest cost burdens (32 % each). Despite this strong NPV,

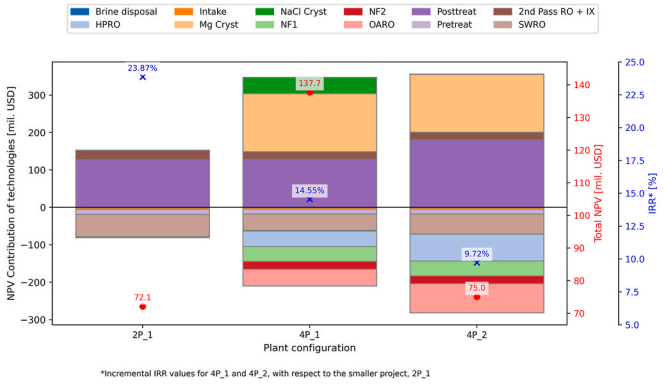

Fig. 6. NPV contribution of technologies (stacked bar plots, primary y-axis) in million USD along with their total (red scatter plots, secondary y-axis) for the three desalination configurations. Also shown are the IRRs for these configurations (blue scatter plots, tertiary y-axis).

its incremental IRR declined to ~14.5 %, reflecting a reduced return on additional investment relative to 2P_1.

In the maximized MLD configuration (4P_2), NPV declined to 75 million USD and IRR dropped further to 9.72 %, only slightly above the 8.75 % discount rate. The 4P_2's underperformance relative to 4P_1 stemmed from much higher cost burdens of OARO and HPRO (104 % and 95 % of NPV, respectively). The NaCl crystallizer's contribution collapsed from 32 % in 4P_1 to just 1 % (due to the higher CSSF), whereas post-treatment rose sharply from 93 % to 240 % due to greater water recovery.

Overall, higher brine valorization reduced rates of return, though MLD configurations still outperformed conventional desalination in total returns. Among them, 4P_1 clearly dominated 4P_2 in both NPV and IRR.

3.6. Sensitivity analysis of financial parameters: increased sensitivity with higher mineral recovery

Fig. 7 shows tornado plots showing the effect of ±50 % variations in six key financial parameters on the NPVs of the two MLD configurations, with base-case NPVs indicated by dashed lines. The conventional configuration (2P_1) is excluded to focus on risks specific to MLD investments.

The base MLD configuration (4P_1) exhibited a narrower NPV range, indicating greater robustness, while the maximized MLD configuration (4P_2) showed higher sensitivity and larger downside risks. $Mg(OH)_2$ revenue alone could shift NPV by ±132 % for 4P_1 and ± 243.5 % for 4P_2, while NaCl revenue could alter NPV by ±77 % and ±172 %, respectively. Potable water revenue had a relatively smaller impact. The ±50 % variation in revenues of these products can also be interpreted as a corresponding variation in their assumed specific prices (see Table 4), assuming that other variables remain constant.

Changes in WACC produced asymmetric effects: a 50 % decrease boosted NPV by 129 % (4P_1) and 244 % (4P_2), whereas a 50 % increase reduced NPV by 68 % and 129 %. This reflects the amplified effect of discounting on later cash flows in more capital- and energy-intensive systems. Other critical parameters included the COGS of the magnesium crystallizer (mainly NaOH cost) and the capital investment of the NaCl crystallizer.

Overall, reusing the magnesium crystallizer's effluent in 4P_2 increased NPV sensitivity, making its financial viability more vulnerable to fluctuations in revenues, costs, and discount rates compared to the base MLD setup.

3.7. Sensitivity analysis for 4P_2's financial parity

Financial parity between 4P_2 and 4P_1 was assessed via two scenarios: increasing 4P_1's BDC or reducing 4P_2's WACC (Fig. 8). In both cases, NPV exhibited a non-linear response due to the discounting of future cash flows.

In summary, 4P_2 can reach financial parity with 4P_1 either through significantly higher BDCs applied to 4P_1 or through reduced WACC for 4P_2, while retaining its advantage in brine minimization.

3.8. Discussion and comparison of results with the literature

This section contextualizes the study's results and methodology against literature benchmarks (summarized in Table 5), highlighting environmental, technical, and financial performance. The study's goal was to identify a desalination configuration that minimizes environmental impact while maintaining financial viability.

3.8.1. Environmental performance

Water recovery, as a measure of brine minimization, was 60.4 % for the conventional 2P_1 configuration, consistent with reported two-stage SWRO values (60–65 % [52]). Recovery increased to 71.4 % in 4P_1, exceeding Sharkh et al. (2023)'s 65.2 % for a similar setup [13], due to additional recovery from the NaCl crystallizer. The magnesium crystallizer was the main limitation, discharging most NF2 retentate. Reusing this effluent in 4P_2, following Morgante et al. [24], raised recovery to 96.7 %, comparable to

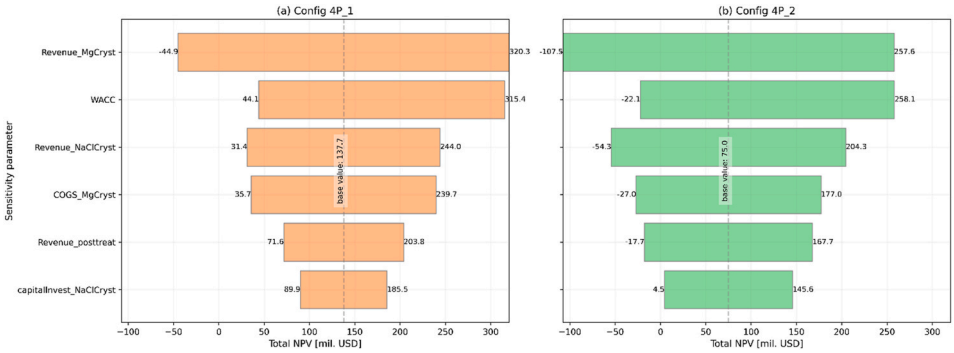

Fig. 7. Tornado plots of NPV sensitivity for the two MLD configurations: (a) 4P_1 and (b) 4P_2. Six key parameters were varied by ±50 %; dashed lines show base NPVs. Abbreviations: capitalInvest = initial capital investment; COGS = cost of goods sold; posttreat = post-treatment; WACC = weighted average cost of capital or discount rate.

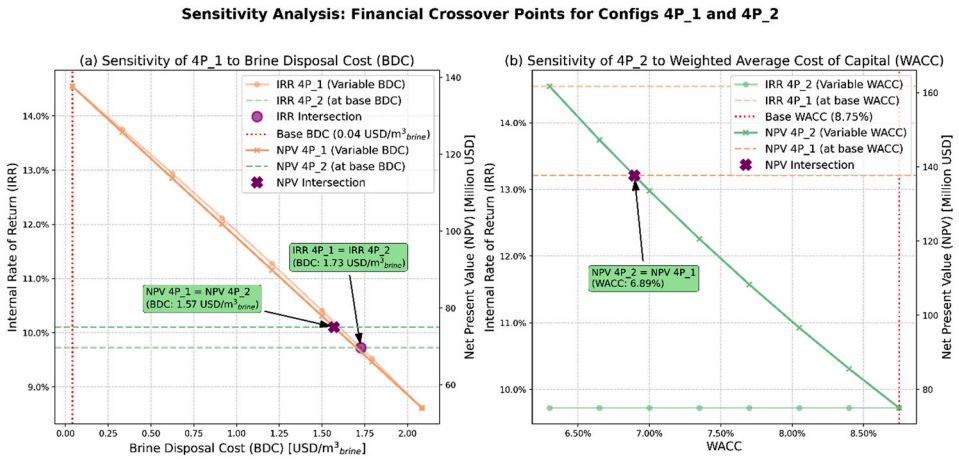

Fig. 8. Comparison of financial measures to achieve financial parity of configuration 4P_2 with 4P_1 by: (a) increasing the BDC for 4P_1 on its IRR and NPV; and (b) decreasing the 4P_2 project's WACC on its IRR and NPV.

- **BDC adjustment** (Fig. 8 (a)): Raising 4P_1's BDC from 0.04 to 1.57 USD/m^3_{brine} aligned its NPV with that of 4P_2, while a BDC of 1.73 $USD/\ m^3_{brine}$ was required for IRR parity. This higher BDC requirement for IRR parity as compared to that for NPV is due to the inherent investment assumptions: for IRR parity, 4P_1's discount rate is set to the IRR of 4P_2 (9.72 %), which is higher than that used for NPV parity (8.75 %), the MLD project's WACC. However, NPV-based parity is more realistic for investment decisions, as it reflects real-world financing conditions [51]. Nevertheless, these BDC levels far exceed typical surface discharge costs (0.05–0.30 USD/m^3_{brine} [12]), making 4P_1 economically less attractive and favoring the MLD-maximizing 4P_2 configuration.
- **WACC reduction** (Fig. 8 (b)): Lowering 4P_2's WACC from 8.75 % to 6.89 % was sufficient to achieve NPV parity, though IRR remained unchanged.

Table 5
Comparison of own results with literature

Parameter	Configuration	Own results	Literature values
Water recovery [%]	2P_1	60.4 %	60–65 % [52]
	4P_2	96.7 %	99 % (BCr) and 86 % (WAIV) [11]
NaCl crystallizer feed impurity [$\frac{mg_{impurities}}{L_{brine}}$]	4P_1	4.0	8.0 (solution mining) [42]
	4P_2	14.7	
NaCl concentration at the feed of NaCl crystallizer [g_{NaCl}/kg_{sol}]	4P_1	146.7	250 (commercial [42]), 200 [42], 242 [23], 192 [25] (assuming a density of 1.17 kg/L), 158 [53] (assuming a density of 1.13 kg/L)
	4P_2	143.0	
SEC [kWh_{el}/m^3_{perm}]	2P_1	3.8	2.5–4.0 [54]
	4P_1	5.84[a]	6.9 [13]
	4P_2	12.2	22.0 [11]
DALC or production cost of potable water [USD/m^3]	4P_1	0.94	0.57 [13]
DALC or production cost of NaCl [USD/ton]	4P_1	27.83[b]	28.87 [13]

[a] Excluding $Mg(OH)_2$ and NaCl crystallizers and second-pass RO with IX.
[b] Excluding NaCl crystallizer share.

Panagopoulos (2022) (BCr: 99 %, WAIV: 86 % [11]), though at the cost of reduced downstream NaCl crystallizer performance. Notably, higher water recovery results in more concentrated brine, necessitating enhanced outfall design and discharge diffusion systems compared with conventional desalination to achieve equivalent dilution levels and mitigate potential adverse impacts on marine biota [55].

3.8.2. NaCl crystallizer performance

NaCl crystallizer efficiency was constrained by feed purity and salinity. Effluent reuse in 4P_2 increased impurities (14.7 vs 4.0 $\frac{mg_{impurities}}{L_{brine}}$ in 4P_1), exceeding solution-mining brines (8.0 $\frac{mg_{impurities}}{L_{brine}}$ [42]). Moreover, simulating alternative feedwater sources from the MENA region showed that effluent reuse in 4P_2 had a stronger impact than feedwater source (see Appendix C.2). Feed salinity in both MLD cases (143–147 g_{NaCl}/kg_{sol}) was below that in commercial systems (250 g_{NaCl}/kg_{sol} [42]) and other ED/ED + MED setups (200–242 g_{NaCl}/kg_{sol} [23,42]). These factors nearly doubled the SEC and capital costs in 4P_2 as compared to commercial systems. Notably, the world's first large-scale OARO commercial plant in Indonesia (178.9 g_{NaCl}/L_{sol} or ~158 g_{NaCl}/kg_{sol} [53]) and alternative NF-MBC pilot systems in more recent publications (225 g_{NaCl}/L_{sol} or ~192 g_{NaCl}/kg_{sol} [25]) have achieved higher NaCl concentrations at the

crystallizer feed than in this study.

3.8.3. Energy and emissions

Although the NaCl crystallizer is highly energy-intensive [23,24], overall SEC aligned with literature. The 2P_1 case consumed 3.8 kWh_{el}/m^3_{perm}, within typical SWRO ranges (2.5–4.0 [54]). Excluding crystallizers and second-pass RO + IX, 4P_1's SEC (5.84 kWh_{el}/m^3_{perm}) was comparable to Sharkh et al. (2023)'s 6.9 kWh_{el}/m^3_{perm} [13]. 4P_2 consumed 12.2 kWh_{el}/m^3_{perm}, still 44 % lower than Panagopoulos (2022)'s BCr chain (22.0 kWh_{el}/m^3_{perm} [11]). Given Morocco's fossil-heavy grid (72 % coal + gas in 2023 [56]), emissions are high: ~8.9 kg CO_2-eq per m^3 of permeate in the 4P_2 case (assuming 0.729 kg CO_2-eq/kWh_{el} [57]).

3.8.4. Scaling and product purity

High divalent ion concentration in NF1 and NF2 retentates posed a gypsum ($CaSO_4$) scaling risk. The Davies equation is unreliable at high ionic strength (>0.5 mol/L), so the Pitzer model in PHREEQC [58] was applied for more accurate prediction. Gypsum saturation index in NF2 retentate was 0.04 (i.e., slight supersaturation at 110 %, $10^{0.04} \cong 1.10$), well below the 250–400 % threshold for effective antiscalant use [13]. $Mg(OH)_2$ precipitation benefited from lower solubility than $Ca(OH)_2$, allowing >95 % purity—suitable for low-grade flame retardants [59]—at pH ~10 (vs. ~12 for $Ca(OH)_2$), provided pH was controlled.

3.8.5. Financial performance and DALC

DALC provided realistic product costs by avoiding distortions from co-product revenue. UPW DALC in 4P_1 was 1.67 USD/m^3 (vs. market price 2.5 USD/m^3 [50]), whereas conventional LC gave −13.1 USD/m^3. NaCl DALC (27.83 USD/ton) closely matched literature for a similar plant setup (28.87 USD/ton in Ref. [13]), confirming method validity.

NPV and IRR analysis confirmed financial viability: 2P_1 had the highest IRR (23.87 %), while 4P_1 and 4P_2 yielded positive NPVs (137.7 and 75.0 million USD) but lower IRRs (14.5 % and 9.7 %). Financial parity for MLD-maximizing 4P_2 could be achieved by increasing 4P_1's BDC ≥1.57 USD/m^3_{brine} or reducing 4P_2's WACC to 6.89 %. Sensitivity analysis identified $Mg(OH)_2$ and NaCl revenues, WACC, and NaOH costs as the most influential factors, consistent with literature [23,24,60].

3.8.6. Scalability

The modeled 2000 m^3/h feed intake can be linearly scaled to larger urea plants (e.g., 1.73 $Mt_{urea}/year$ requiring ~2723 m^3/h [7]), within commercial capacities for similar MLD configurations (4195 m^3_{feed}/h [13]), suggesting feasible industrial implementation.

4. Conclusions and future work

This study evaluated alternative desalination configurations to meet the freshwater requirements of a hypothetical 1.27 $Mt_{urea}/year$ decarbonized urea plant located on Morocco's Mediterranean coast, requiring 641.4 m^3/h of potable water and 160.35 m^3/h of ultrapure water (UPW). A conventional seawater reverse osmosis system (2P_1) was compared against two minimum liquid discharge (MLD) configurations designed to additionally recover magnesium hydroxide ($Mg(OH)_2$) and sodium chloride (NaCl). The MLD-maximizing configuration (4P_2) incorporated reuse of the magnesium crystallizer effluent to further reduce brine generation relative to the base MLD setup (4P_1). The objective was to identify the configuration offering the most favorable environmental and techno-economic performance. The financial assessment employed net present value (NPV), internal rate of return (IRR), levelized cost (LC), and a novel indicator—the discounted and allocated LC (DALC)—which excludes revenue from co-products.

The findings, addressing the research questions outlined in Section 1.2, are summarized as follows:

1. **Environmental impacts:** Configuration 4P_2 achieved the highest brine reduction relative to 2P_1 (88 % vs. 22.7 % in 4P_1) and the greatest total water recovery (96.7 % compared with 71.4 % and 60.4 % for 4P_1 and 2P_1, respectively). These gains were offset by lower NaCl crystallizer efficiency, reflected in a higher purge ratio (21.3 % vs 5.8 % in 4P_1). The specific electricity consumption (SEC) of both the MLD configurations was approximately three times higher than that of 2P_1, highlighting the trade-offs between brine minimization and energy demand.
2. **Economic viability:** Among the three schemes, 4P_2 exhibited the highest water DALC, driven by the additional costs associated with recycling the magnesium crystallizer effluent, whereas 2P_1 had the lowest. In contrast, 4P_1 yielded the lowest conventional LC, benefiting from mineral recovery while avoiding the incremental costs of MLD maximization in 4P_2. Although the IRR was highest for the conventional configuration (2P_1), the total project returns (NPV) were most favorable for 4P_1—exceeding those of both 2P_1 and 4P_2 by more than 80 %. Notably, 4P_2's NPV was only marginally higher that of the conventional configuration (75 vs. 72.1 million USD), despite incorporating additional mineral revenue streams. This outcome primarily reflects the cost drag arising from higher brine volume handling due to effluent reuse from the magnesium crystallizer across its energy-intensive units, such as high-pressure reverse osmosis (HPRO), osmotically-assisted RO (OARO).
3. **Sensitivity:** The NPV of MLD configurations was most sensitive to changes in $Mg(OH)_2$ revenue and the weighted average cost of capital (WACC). Configuration 4P_2 displayed greater sensitivity and higher downside risk. Financial parity between the MLD-maximizing configuration (4P_2) and the financially best-performing configuration (4P_1) could be achieved by either increasing the brine disposal cost for 4P_1 from 0.04 to 1.57 USD/m^3_{brine} or by reducing 4P_2's WACC from 8.75 % to 6.89 %.

The study thus met its objective of identifying the environmentally and financially preferred configuration: 4P_2 emerged as the most suitable option in terms of brine minimization and water recovery, achieving financial parity with 4P_1 when supported by favorable project financing or higher brine disposal costs.

Some key takeaways from the study:

- Ensuring high feed purity to the NaCl crystallizer is critical to minimize energy consumption and capital expenditure penalties.
- Strategic project financing mechanisms—such as preferential capital costs or targeted subsidies—can substantially enhance the financial viability of MLD-maximizing configurations. Likewise, implementing brine discharge levies or effluent charges can discourage lower-recovery designs by internalizing the environmental costs of brine disposal.

4.1. Future research directions

Based on the results from this study, the following suggestions are made:

1. Develop more effective removal strategies for divalent ions (Ca^{2+}, SO_4^{2-}) from the nanofiltration retentate prior to crystallization to improve mineral purity and process efficiency.
2. Standardize the DALC-based cost allocation framework for complex desalination and mineral recovery systems [61].
3. Investigate advanced brine concentration methods and energy-efficient NaCl crystallizer technologies to lower SEC and enable higher feed salinities ($>147\ g_{NaCl}/kg_{sol}$).
4. Conduct comprehensive life-cycle assessments (LCA) to evaluate the environmental implications of MLD strategies relative to conventional desalination and traditional mineral extraction routes.
5. Explore pathways for retrofitting existing desalination plants with MLD units utilizing concentrated brine streams, thereby reducing the investment and risks associated with greenfield deployment [24].

These directions aim to support researchers, plant operators, and policymakers in advancing sustainable and financially viable MLD-based desalination for industrial water reuse and resource recovery.

CRediT authorship contribution statement

Nikhil Dilip Pawar: Writing – review & editing, Writing – original draft, Visualization, Validation, Methodology, Investigation, Formal analysis, Conceptualization. **Carmelo Morgante:** Writing – review & editing, Writing – original draft, Visualization, Methodology, Conceptualization. **Thomas Pregger:** Writing – review & editing, Funding acquisition, Conceptualization. **Patrick Jochem:** Writing – review & editing, Conceptualization.

Declaration of generative AI and AI-assisted technologies in the writing process

During the preparation of this work the authors used ChatGPT in order to improve readability and language. After using this tool, the authors reviewed and edited the content as needed and take full responsibility for the content of the publication.

Declaration of competing interest

The authors declare the following financial interests/personal relationships which may be considered as potential competing interests:Nikhil Dilip Pawar reports financial support was provided by German Aerospace Center DLR. If there are other authors, they declare that they have no known competing financial interests or personal relationships that could have appeared to influence the work reported in this paper.

Appendix A. Supplementary data

Supplementary data to this article can be found online at https://doi.org/10.1016/j.wri.2025.100332.

Data availability

A link to Mendeley Data will be shared at a later stage (currently not shared to allow double-blinded peer review)" with "The simulation results are openly accessible at Mendeley Data, doi: 10.17632/yzy4mcf7tp.1.

References

[1] Samantha Kuzma, Liz Saccoccia, Marlena Chertock, 25 Countries, Housing One-Quarter of the Population, Face Extremely High Water Stress, 2023.
[2] J. Sowers, A. Vengosh, E. Weinthal, Climate change, water resources, and the politics of adaptation in the Middle East and North Africa, Clim. Change 104 (2011) 599–627, https://doi.org/10.1007/s10584-010-9835-4.
[3] K. Waha, L. Krummenauer, S. Adams, V. Aich, F. Baarsch, D. Coumou, M. Fader, H. Hoff, G. Jobbins, R. Marcus, M. Mengel, I.M. Otto, M. Perrette, M. Rocha, A. Robinson, C.-F. Schleussner, Climate change impacts in the Middle East and Northern Africa (MENA) region and their implications for vulnerable population groups, Reg. Environ. Change 17 (2017) 1623–1638, https://doi.org/10.1007/s10113-017-1144-2.
[4] S.-H. Lee, R.H. Mohtar, S.-H. Yoo, Assessment of food trade impacts on water, food, and land security in the MENA region, Hydrol. Earth Syst. Sci. 23 (2019) 557–572, https://doi.org/10.5194/hess-23-557-2019.
[5] World Fertilizer, The Middle East in Focus: Part 2, 2018.
[6] Y. Gao, A. Cabrera Serrenho, Greenhouse gas emissions from nitrogen fertilizers could be reduced by up to one-fifth of current levels by 2050 with combined interventions, Nat. Food 4 (2023) 170–178, https://doi.org/10.1038/s43016-023-00698-w.
[7] N.D. Pawar, K. Singhal, C. Bhushan, T. Pregger, P. Jochem, Decarbonization of urea production in India and its impact on water withdrawal and costs: a cost optimization approach, J. Clean. Prod. 486 (2025) 144433, https://doi.org/10.1016/j.jclepro.2024.144433.
[8] R.M. Nayak-Luke, L. Hatton, Z. Cesaro, R. Bañares-Alcántara, Assessing the viability of decarbonising India's nitrogenous fertiliser consumption, J. Clean. Prod. 366 (2022) 132462, https://doi.org/10.1016/j.jclepro.2022.132462.
[9] E. Jones, M. Qadir, M.T.H. van Vliet, V. Smakhtin, S.-M. Kang, The state of desalination and brine production: a global outlook, Sci. Total Environ. 657 (2019) 1343–1356, https://doi.org/10.1016/j.scitotenv.2018.12.076.
[10] Z. Benjelloun, K. Saoud, Phosphate mining and the circular economy: Morocco's OCP Group's approach to sustainable water use, in: C. Davis, E. Rosenblum (Eds.), Sustainable Industrial Water Use: Perspectives, Incentives, and Tools, IWA Publishing, 2021, pp. 63–72.
[11] A. Panagopoulos, Techno-economic assessment of zero liquid discharge (ZLD) systems for sustainable treatment, minimization and valorization of seawater brine, J. Environ. Manag. 306 (2022) 114488, https://doi.org/10.1016/j.jenvman.2022.114488.
[12] A. Panagopoulos, K.-J. Haralambous, M. Loizidou, Desalination brine disposal methods and treatment technologies - a review, Sci. Total Environ. 693 (2019) 133545, https://doi.org/10.1016/j.scitotenv.2019.07.351.
[13] A.-A. Sharkh, S. Ihm, A.M. Farooque, E.S. Al-Waznani, N. Voutchkov, Dual brine concentration for the beneficial use of two concentrate streams from desalination plant - concept proposal and pilot plant demonstration, Desalination 564 (2023) 116789, https://doi.org/10.1016/j.desal.2023.116789.
[14] A. Panagopoulos, Brine management (saline water & wastewater effluents): sustainable utilization and resource recovery strategy through Minimal and Zero Liquid Discharge (MLD & ZLD) desalination systems, Chem. Eng. Process. Process Intensif. 176 (2022) 108944, https://doi.org/10.1016/j.cep.2022.108944.
[15] N.D. Pawar, H.U. Heinrichs, C. Winkler, P.-M. Heuser, S.D. Ryberg, M. Robinius, D. Stolten, Potential of green ammonia production in India, Int. J. Hydrogen Energy 46 (2021) 27247–27267, https://doi.org/10.1016/j.ijhydene.2021.05.203.
[16] B.A. Sharkh, A.A. Al-Amoudi, M. Farooque, C.M. Fellows, S. Ihm, S. Lee, S. Li, N. Voutchkov, Seawater desalination concentrate—a new frontier for sustainable mining of valuable minerals, npj Clean Water 5 (2022), https://doi.org/10.1038/s41545-022-00153-6.
[17] P. Ortiz-Albo, S. Torres-Ortega, M. González Prieto, A. Urtiaga, R. Ibañez, Techno-economic feasibility analysis for minor elements valorization from desalination concentrates, Separ. Purif. Rev. 48 (2019) 220–241, https://doi.org/10.1080/15422119.2018.1470537.
[18] A. Del Villar, J. Melgarejo, M. García-López, P. Fernández-Aracil, B. Montano, The economic value of the extracted elements from brine concentrates of Spanish desalination plants, Desalination 560 (2023) 116678, https://doi.org/10.1016/j.desal.2023.116678.
[19] G. Al Bazedi, R.S. Ettouney, S.R. Tewfik, M.H. Sorour, M.A. El-Rifai, Salt recovery from brine generated by large-scale seawater desalination plants, Desalination Water Treat. 52 (2014) 4689–4697, https://doi.org/10.1080/19443994.2013.810381.
[20] W. Zhang, M. Miao, J. Pan, A. Sotto, J. Shen, C. Gao, B. van der Bruggen, Process economic evaluation of resource valorization of seawater concentrate by membrane technology, ACS Sustainable Chem. Eng. 5 (2017) 5820–5830, https://doi.org/10.1021/acssuschemeng.7b00555.
[21] M. Micari, M. Moser, A. Cipollina, B. Fuchs, B. Ortega-Delgado, A. Tamburini, G. Micale, Techno-economic assessment of multi-effect distillation process for the treatment and recycling of ion exchange resin spent brines, Desalination 456 (2019) 38–52, https://doi.org/10.1016/j.desal.2019.01.011.
[22] D. von Eiff, P.W. Wong, Y. Gao, S. Jeong, A.K. An, Technical and economic analysis of an advanced multi-stage flash crystallizer for the treatment of concentrated brine, Desalination 503 (2021) 114925, https://doi.org/10.1016/j.desal.2020.114925.
[23] N.D. Pawar, S. Harris, K. Mitko, G. Korevaar, Valorization of coal mine effluents — challenges and economic opportunities, Water Resour. Ind. 28 (2022) 100179, https://doi.org/10.1016/j.wri.2022.100179.
[24] C. Morgante, F. Vassallo, D. Xevgenos, A. Cipollina, M. Micari, A. Tamburini, G. Micale, Valorisation of SWRO brines in a remote island through a circular approach: techno-economic analysis and perspectives, Desalination 542 (2022) 116005, https://doi.org/10.1016/j.desal.2022.116005.
[25] A.S. Abdalrhman, S. Ihm, E.S. Alwaznani, C.M. Fellows, S. Li, S. Lee, A.S. Al-Amoudi, A.M. Farooque, N. Voutchkov, Novel nanofiltration-reverse osmosis-high pressure nanofiltration membrane brine concentration (NF-RO-HPNF MBC) system for producing high purity high concentration sodium chloride brine from seawater, Desalination 597 (2025) 118308, https://doi.org/10.1016/j.desal.2024.118308.
[26] NREL, Simple Levelized Cost of Energy (LCOE) calculator documentation. https://www.nrel.gov/analysis/tech-lcoe-documentation.html, 2025. (Accessed 15 April 2025).
[27] N. Salmon, R. Bañares-Alcántara, Offshore green ammonia synthesis, Nat. Synth. 2 (2023) 604–611, https://doi.org/10.1038/s44160-023-00309-3.
[28] A. Kakavand, S. Sayadi, G. Tsatsaronis, A. Behbahaninia, Techno-economic assessment of green hydrogen and ammonia production from wind and solar energy in Iran, Int. J. Hydrogen Energy 48 (2023) 14170–14191, https://doi.org/10.1016/j.ijhydene.2022.12.285.
[29] H. Ishaq, M.F. Shehzad, C. Crawford, Transient modeling of a green ammonia production system to support sustainable development, Int. J. Hydrogen Energy 48 (2023) 39254–39270, https://doi.org/10.1016/j.ijhydene.2023.07.036.
[30] M. Müller, M. Pfeifer, D. Holtz, K. Müller, Comparison of green ammonia and green hydrogen pathways in terms of energy efficiency, Fuel 357 (2024) 129843, https://doi.org/10.1016/j.fuel.2023.129843.
[31] Lenntech, Major ion composition of seawater. https://www.lenntech.com/composition-seawater.htm, 2025. (Accessed 26 February 2025).
[32] S.G. Simoes, J. Catarino, A. Picado, T.F. Lopes, S. Di Berardino, F. Amorim, F. Gírio, C.M. Rangel, T. Ponce de Leão, Water availability and water usage solutions for electrolysis in hydrogen production, J. Clean. Prod. 315 (2021) 128124, https://doi.org/10.1016/j.jclepro.2021.128124.
[33] EUROWATER, Water Treatment for Green Hydrogen, 2024.
[34] M. Badruzzaman, N. Voutchkov, L. Weinrich, J.G. Jacangelo, Selection of pretreatment technologies for seawater reverse osmosis plants: a review, Desalination 449 (2019) 78–91, https://doi.org/10.1016/j.desal.2018.10.006.
[35] G. Amy, N. Ghaffour, Z. Li, L. Francis, R.V. Linares, T. Missimer, S. Lattemann, Membrane-based seawater desalination: present and future prospects, Desalination 401 (2017) 16–21, https://doi.org/10.1016/j.desal.2016.10.002.
[36] M. Ginsberg, Z. Zhang, A.A. Atia, M. Venkatraman, D.V. Esposito, V.M. Fthenakis, Integrating solar energy, desalination, and electrolysis, Sol. RRL 6 (2022) 2100732, https://doi.org/10.1002/solr.202100732.
[37] D. Zhou, L. Zhu, Y. Fu, M. Zhu, L. Xue, Development of lower cost seawater desalination processes using nanofiltration technologies — a review, Desalination 376 (2015) 109–116, https://doi.org/10.1016/j.desal.2015.08.020.
[38] L. Llenas, G. Ribera, X. Martínez-Lladó, M. Rovira, J. de Pablo, Selection of nanofiltration membranes as pretreatment for scaling prevention in SWRO using real seawater, Desalination Water Treat. 51 (2013) 930–935, https://doi.org/10.1080/19443994.2012.714578.
[39] S. Romano, S. Trespi, R. Achermann, G. Battaglia, A. Raponi, D. Marchisio, M. Mazzotti, G. Micale, A. Cipollina, The role of operating conditions in the precipitation of magnesium hydroxide hexagonal platelets using NaOH solutions, Cryst. Growth Des. 23 (2023) 6491–6505, https://doi.org/10.1021/acs.cgd.3c00462.

[40] M. Micari, D. Diamantidou, B. Heijman, M. Moser, A. Haidari, H.S. panjers, V. Bertsch, Experimental and theoretical characterization of commercial nanofiltration membranes for the treatment of ion exchange spent regenerant, J. Membr. Sci. 606 (2020) 118117, https://doi.org/10.1016/j.memsci.2020.118117.
[41] B. van der Bruggen, K. Everaert, D. Wilms, C. Vandecasteele, Application of nanofiltration for removal of pesticides, nitrate and hardness from ground water: rejection properties and economic evaluation, J. Membr. Sci. 193 (2001) 239–248, https://doi.org/10.1016/S0376-7388(01)00517-8.
[42] K.G. Nayar, J. Fernandes, R.K. McGovern, K.P. Dominguez, A. McCance, B.S. Al-Anzi, J.H. Lienhard, Cost and energy requirements of hybrid RO and ED brine concentration systems for salt production, Desalination 456 (2019) 97–120, https://doi.org/10.1016/j.desal.2018.11.018.
[43] N. Voutchkov, Desalination Project Cost Estimating and Management, CRC Press, Boca raton Taylor & Francis, a CRC Title, Part of the Taylor & Francis Imprint, a Member of the Taylor & Francis Group, the Academic Division of T&F Informa, Plc, 2018, 2018.
[44] R.A. Brealey, S.C. Myers, F. Allen, Principles of Corporate Finance, McGraw-Hill Education, thirteenthth Edition, 2019.
[45] PWC, Morocco - corporate - significant developments. https://taxsummaries.pwc.com/morocco/corporate/, 2024. (Accessed 27 January 2025).
[46] Marshad Bin, Mohammed H. Saud, Economic evaluation of seawater desalination a case study analysis of cost of water production from seawater desalination in Saudi Arabia, Doctor Philos. Water Res. (2014).
[47] H. El Hafdaoui, A. Khallaayoun, S. Al-Majeed, Renewable energies in Morocco: a comprehensive review and analysis of current status, policy framework, and prospective potential, Energy Convers. Manag. X 26 (2025) 100967, https://doi.org/10.1016/j.ecmx.2025.100967.
[48] Salary Explorer, Chemical plant operator average salary in Morocco 2024. https://www.salaryexplorer.com/average-salary-wage-comparison-morocco-chemical-plant-operator-c146j12174, 2024. (Accessed 18 February 2025).
[49] S.A. Wheeler, C. Nauges, R.Q. Grafton, Water Pricing, Costs and Markets, 2023.
[50] A.F. Ismail, K.C. Khulbe, T. Matsuura, Reverse Osmosis, Elsevier, Amsterdam Netherlands, Cambridge MA, 2019.
[51] L. Bakić, Internal rate of return in project management: IRR formula & examples. https://productive.io/blog/internal-rate-of-return-in-project-management/#:~:text=4.,reinvestment%2Drate%20assumption%20can%20be%3A, 2025. (Accessed 8 August 2025).
[52] J. Kim, K. Park, S. Hong, Optimization of two-stage seawater reverse osmosis membrane processes with practical design aspects for improving energy efficiency, J. Membr. Sci. 601 (2020) 117889, https://doi.org/10.1016/j.memsci.2020.117889.
[53] AquaEnergy Expo, AquaEnergy Expo Magazine-12th-Issue-December2024, 2024.
[54] N. Voutchkov, Desalinated water, in: M. Qadir, V. Smakhtin, S. Koo-Oshima, E. Guenther (Eds.), Unconventional Water Resources, Springer International Publishing, Cham, 2022, pp. 233–254.
[55] N. Voutchkov, Overview of seawater concentrate disposal alternatives, Desalination 273 (2011) 205–219, https://doi.org/10.1016/j.desal.2010.10.018.
[56] IEA, Morocco - Countries & Regions -, IEA, 2025. https://www.iea.org/countries/morocco/electricity. (Accessed 18 February 2025).
[57] Scopes data, Morocco | sustainability country information. https://scopesdata.com/sustainability-country-information/morocco-2023#:~:text=With%20a%20national%20electricity%20emission,fuel%20dependence%20for%20electricity%20generation, 2025. (Accessed 22 August 2025).
[58] D.L. Parkhurst, C.A.J. Appelo, Description of input and examples for PHREEQC version 3—A computer program for speciation, batch-reaction. One-Dimensional Transport, and Inverse Geochemical Calculations, U.S. Geological Survey, Reston, VA, 2013.
[59] C. Morgante, T. Moghadamfar, J. Lopez, J.L. Cortina, A. Tamburini, Evaluation of enhanced nanofiltration membranes for improving magnesium recovery schemes from seawater/brine: integrating experimental performing data with a techno-economic assessment, J. Environ. Manag. 360 (2024) 121192, https://doi.org/10.1016/j.jenvman.2024.121192.
[60] M. Micari, A. Cipollina, A. Tamburini, M. Moser, V. Bertsch, G. Micale, Techno-economic analysis of integrated processes for the treatment and valorisation of neutral coal mine effluents, J. Clean. Prod. 270 (2020) 122472, https://doi.org/10.1016/j.jclepro.2020.122472.
[61] S.M. Datar, M.V. Rajan, Cost Accounting: a Managerial Emphasis, seventeenth ed., Pearson, Harlow, United Kingdom, 2021.